Journal of Southeast University (English Edition) Vol. 32, No. 4, pp. 489 - 495 Dec. 2016 ISSN 1003—7985

Experiment and numerical simulation on flow and heat transfer in all-glass evacuated tube solar collectors

Zhang Tao Han Jitian Chen Changnian Kong Lingjian Liu Yang

(School of Energy and Power Engineering, Shandong University, Jinan 250061, China)

Abstract: The experimental study of natural convection in all-glass evacuated tube solar collectors is performed through the experimental platform of the solar-assisted fuel cell system. The experimental facility includes solar collectors with different length and diameter tubes, different coating materials, and with/without guide plates, respectively. Three-dimensional mathematical models on natural and forced convections in the solar collectors are established and the experimental data is validated by field synergy and entransy principles. The results of natural convection show that the water temperature increases and thermal efficiency decreases gradually with the evacuated tube length. The thermal efficiency increases when absorption rates increase from 0.95 to 1.0 and emission rates decrease from 0.16 to 0.06. The thermal efficiency of solar collectors is increased after being equipped with the guide plate, which is attributed to the disappearance of the mixed flow and the enhancement of the heat transfer at the bottom of the evacuated tube. The results of forced convertion indicate that the Reynolds, Nusselt and entransy increments of the horizontal double collectors are higher than those of the vertical single collector while the entransy dissipation is lower than that of the vertical single collector. It is concluded that the solar collectors with guide plates are suitable for natural convection while the double horizontal collectors are suitable for forced convection in the thermal field of solar-assisted fuel cell systems with low and medium temperatures.

Key words: all-glass evacuated tube solar collectors; the solar-assisted fuel cells; field synergy principle; entransy dissipation

DOI: 10.3969/j.issn.1003-7985.2016.04.016

Solar energy is a type of renewable energy and it plays a significant role in saving conventional energy and protecting the environment. Fuel cells are the most efficient means to directly convert the chemical energy stored in fuels to electrical energy through an electrochemical reaction in an isothermal process. As a result, the solar energy coupled with fuel cell technology will be one of the most promising options for the future green energy solutions due to its high efficiency and environmental friendliness[1-2]. PV panels and batteries along with an electrolyser/hydrogen tank and the fuel cell can form a hybrid power generation system called the solar-assisted fuel cell system (SAFCS)[3]. In order to improve the entire energy efficiency of the SAFCS, it is crucially important to enhance the thermal performance of the all-glass evacuated tube solar system. The simulation results of a single tube water heater indicate that there is a stagnation zone at the bottom of the evacuated tube and a random vortex at the junction of the water tank, thus reducing the heat transfer efficiency of the evacuated tube. However, when the vortex disappears and the flow becomes stable, the heat transfer efficiency increases while the evacuated tube is equipped with guide plates[4-7]. Therefore, it is an effective way to use the guide plate to enhance the heat transfer in the solar water heater. The experimental results show that when the water temperature exceeds 45 ℃, the system efficiency will be 0.49 to 0.57 if the evacuated tube length, water tank volume and insulation thickness are reasonably allocated[8-9].

On the basis of the above-mentioned research, in order to develop the SAFCS, the solar water heaters of different tube lengths, diameters, coating materials and guide plates are studied by using the FLUENT and the experimental platform of the SAFCS. The simulation results are compared with the experimental data in detail. The effects of tube lengths, diameters, coating materials and guide plates on the heat transfer performance of all-glass evacuated tube solar water heaters are further analyzed by using field synergy and entransy methods.

1 Models and Simulation Method

1.1 Mathematical models

The all-glass evacuated tube solar collector is mainly composed of a water tank, insulation layer, inner glass tube, cover glass tube, support pieces, getter, reflector and guide plate. In the simulation process, the initial conditions for velocities are set to be $u=0$, $v=0$ and $w=0$ with all solid walls having no slip boundary while the PISO operator and DO radiation model are adopted. The

Received 2016-05-18.

Biographies: Zhang Tao(1974—), male, doctor; Han Jitian(corresponding author), male, doctor, professor, jthan@sdu.edu.cn.

Foundation items: The National Natural Science Foundation of China (No. 51376110, 51541604), the Major International (Regional) Joint Research Project of the National Natural Science Foundation of China (No. 61320106011).

Citation: Zhang Tao, Han Jitian, Chen Changnian, et al. Experiment and numerical simulation on flow and heat transfer in all-glass evacuated tube solar collectors[J]. Journal of Southeast University (English Edition), 2016, 32(4): 489 - 495. DOI: 10.3969/j.issn.1003-7985.2016.04.016.

outer wall temperature is regarded as a constant temperature, $T_0 = 293$ K. The evacuated tubes are regarded as overall being cylinder heated. Coating is seen as an internal heating source. The half ball at the end of the glass tube is processed into a flat shape. The Laminar model is adopted for natural convection while the *k*-epsilon turbulence model is used for forced convection. The water heater with reflectors is described as being double heated while the other is single heated, as shown in Fig. 1.

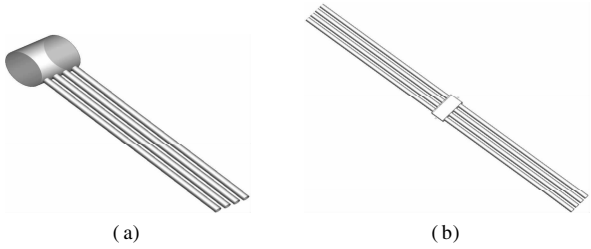

(a) (b)

Fig. 1 Physical and mathematical models for solar collectors. (a) Natural convection heat transfer; (b) Forced convection heat transfer

1.2 Governing equations

The general variable equation is

$$\frac{\delta(\rho\varphi)}{\delta t} + \mathrm{div}(\rho\varphi \boldsymbol{u}) = \mathrm{div}(\boldsymbol{\Gamma} \cdot \mathrm{grad}\varphi) + S_\varphi \quad (1)$$

where ρ is the fluid density, kg/m^3; t is the time, s; φ is the general variable; div is the vector divergence; Γ is the diffusion coefficient; grad is the general variable gradient; S_φ is the general variable source term; $u = u\boldsymbol{i} + v\boldsymbol{j} + w\boldsymbol{z}$, u, v, w are the velocity components in the x, y, z coordinates.

The radiative transfer equation is

$$\frac{\mathrm{d}I(\boldsymbol{r},\boldsymbol{s})}{\mathrm{d}l} + (\alpha+\sigma_\mathrm{c})I(\boldsymbol{r},\boldsymbol{s}) = \alpha n^2 \frac{\sigma T^4}{\pi} + \frac{\sigma_\mathrm{c}}{4\pi}\int_0^{4\pi} I(\boldsymbol{r},\boldsymbol{s}')\phi(\boldsymbol{s},\boldsymbol{s}')\mathrm{d}\Omega' \quad (2)$$

where $\boldsymbol{r}$ is the position vector; $\boldsymbol{s}$ is the direction vector; $\boldsymbol{s}'$ is the scattering direction; l is the one-way length (stroke length); α is the absorption coefficient; n is the refractive index; σ_c is the scattering coefficient; σ is the Stephen-Boltzmann number, W/(m^2 · K^4); I is the radiation intensity depending on position vector $\boldsymbol{r}$ and direction vector $\boldsymbol{s}$; T is the local temperature, K; ϕ is the phase function; Ω' is the space solid angle; and $\alpha + \sigma_\mathrm{c}$ is the medium optical depth.

The standard *k*-ε equation is

$$\frac{\partial(\rho k)}{\partial t} + \frac{\partial(\rho k u_i)}{\partial x_i} = \frac{\partial}{\partial x_j}\left[\left(\mu + \frac{\mu_i}{\alpha_\mathrm{k}}\right)\frac{\partial k}{\partial x_j}\right] + G_\mathrm{k} + G_\mathrm{b} - \rho\varepsilon - Y_\mathrm{M} + S_\mathrm{k} \quad (3)$$

$$\frac{\partial(\rho\varepsilon)}{\partial t} + \frac{\partial(\rho\varepsilon u_i)}{\partial x_i} = \frac{\partial}{\partial x_j}\left[\left(\mu + \frac{\mu_i}{\alpha_\varepsilon}\right)\frac{\partial \varepsilon}{\partial x_j}\right] + C_{1\varepsilon}\frac{\varepsilon}{k}(G_\mathrm{k} + C_{3\varepsilon}G_\mathrm{b}) - C_{2\varepsilon}\rho\frac{\varepsilon^2}{k} + S_\varepsilon \quad (4)$$

where G_k generated by the mean velocity gradient is a turbulent kinetic energy term; G_b caused by buoyancy is a turbulent kinetic energy term; Y_M is the pulse expansion coefficient in the compressible turbulent flow; $C_{1\varepsilon}$, $C_{2\varepsilon}$, $C_{3\varepsilon}$ are the empirical constants; α_ε is the Prandtl number corresponding to dissipation rate ε and α_k is the Prandtl number corresponding to turbulent kinetic energy k; S_k and S_ε are the custom source terms.

1.3 Performance indicators

The collector thermal efficiency η is defined as

$$\eta = \frac{\rho_\mathrm{w} c_\mathrm{pw} v_\mathrm{s}(t_\mathrm{e} - t_\mathrm{b})}{A_\mathrm{c} G} \quad (5)$$

where ρ_w is the water density, kg/m^3; c_pw is the water specific heat, J/(kg · ℃); v_s is the fluid volume in the water tank, m^3; t_e is the end temperature, ℃; t_b is the initial temperature, ℃; A_c is the contour aperture area, m^2; G is the irradiation, W/m^2.

The Reynolds number *Re* is defined as

$$Re = \frac{ud}{\gamma} \quad (6)$$

where u is the average velocity of the evacuated tube outlet, m/s; d is the internal diameter of the evacuated tube, m; and γ is the fluid viscosity, m^2/s.

The Prandtl number *Pr* is expressed as

$$Pr = \frac{c_\mathrm{p}\mu}{\lambda_\mathrm{f}} \quad (7)$$

where c_p is the fluid constant pressure specific heat, kJ/(kg · ℃); μ is the fluid dynamic viscosity, kg/(m · s); λ_f is the thermal conductivity, W/(m · ℃).

The Nusselt number *Nu* is given as

$$Nu = 0.023 Re^{0.8} Pr^{0.4} \quad (8)$$

The entransy variable is written as

$$\Delta E_\mathrm{h} = \int_0^{t_\mathrm{e}} Q_\mathrm{vhe}\mathrm{d}T - \int_0^{t_\mathrm{b}} Q_\mathrm{vhb}\mathrm{d}T = \frac{Mc_\mathrm{ve}t_\mathrm{e}^2}{2} - \frac{Mc_\mathrm{vb}t_\mathrm{b}^2}{2} \quad (9)$$

where ΔE_h is the entransy variable, J · K; M is the object quality, kg; c_v is the constant volume specific heat, J/(kg · K).

The entransy dissipation E_φ is defined as

$$E_\varphi = -q \cdot \nabla T = \lambda_\mathrm{f}(\nabla T)^2 \quad (10)$$

where ∇T is the temperature gradient.

2 Influence Factors

2.1 Experimental devices

The test setup of influence factors for the solar water heater is shown in Fig. 2. The thermal performance tests of solar water heaters are conducted on two types of evacuated tubes in ϕ47 × 1 500 mm and ϕ58 × 1 800 mm with

different absorptivities, emissivities and photovoltaic parameters, and with/without guide plates. Two methods of stagnation and change water are adopted in the test process. The instruments for measuring temperature, humidity, radiation intensity, and wind speed and direction are equipped in the test system and a data acquisition system based on PC is used to collect and process the test data.

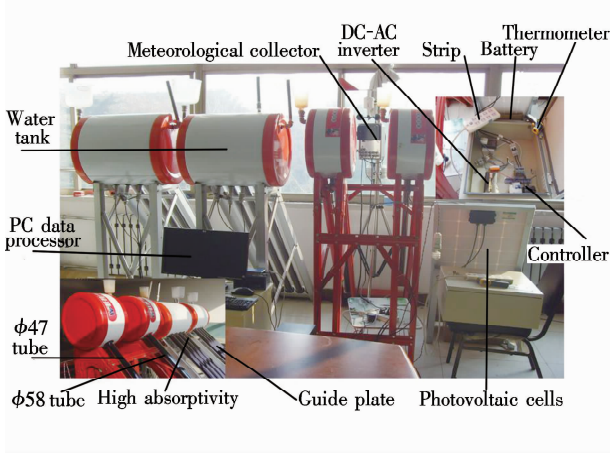

Fig. 2 Experimental platform of natural convection for comprehensive utilization of solar energy

2.2 Tube length and diameter

The test setup is constructed to test the thermal performance of evacuated tube water heaters. The central water temperature is recorded every 10 min with the PT100 thermal resistances installed at the bottom of the water tank. As shown in Fig. 3 (a), the central point temperature of two single tube water heaters gradually increases with the radiant duration of time. Although the central point water temperature of the water tank with a tube of $\phi 58 \times 1\,800$ mm is higher than that of the water tank of $\phi 47 \times 1\,500$ mm during stagnation and change water processes, the thermal efficiency of water heater of $\phi 47 \times 1\,500$ mm is better than that of $\phi 58 \times 1\,800$ mm. The influence of irradiance variation and the tube length with a single or double heated water heater on thermal efficiency are simulated by using the above-developed mathematical model for the evacuated tube. As shown in Fig. 3 (b), the central point temperature of two single tube water heaters gradually rises with irradiation and heated time, but the water temperature of $\phi 58 \times 1\,800$ mm is higher than that of $\phi 47 \times 1\,500$ mm. The entransy increment of two single tube water heaters gradually increases with the tube length, but the entransy increment of $\phi 58$ mm is higher than that of $\phi 47$ mm in the same tube length. The entransy increment for water in the tank with the tube of $\phi 58$ mm heated on double surfaces is higher than that of the single surface. There is a fluctuation at 1 800 mm, but the entransy increment of water in the tank with the tube of $\phi 47$ mm heated on a single surface is higher than that of the double surface.

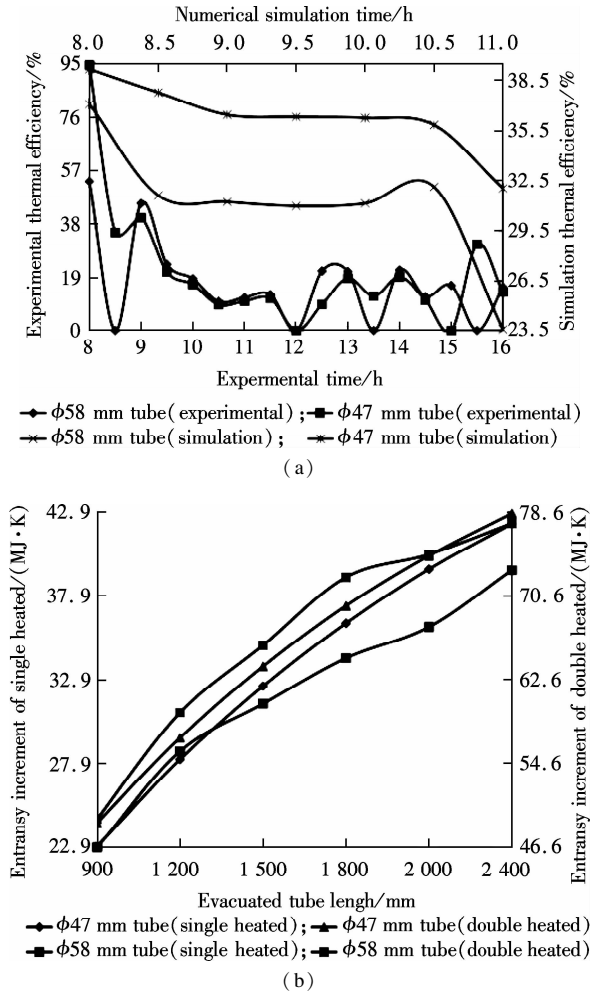

Fig. 3 Simulation analysis of tube diameters and lengths. (a) Thermal efficiency verification; (b) Evacuated tube length

2.3 Absorptivity and emissivity

The solar water heater with the evacuated tube of $\phi 58 \times 1\,800$ mm in different absorptivities and emissivities is used to evaluate the thermal performance. The test results demonstrate that the temperature rise indicates negative growth at the beginning of the stagnation test due to the overnight heat loss, but the temperature rise becomes positive. The heater thermal performance with the tube of high absorptivity is superior to that of low absorptivity. The influences of absorptivity and emissivity on the thermal efficiency of heaters are simulated with the absorptivity ranging from 0.8 to 1.0 and the emissivity from 0.06 to 0.36. As shown in Fig. 4, both entransy increment and thermal efficiency decrease with the increase in absorptivity from 0.85 to 0.95, but increase sharply with the increase in absorptivity from 0.95 to 1.0.

2.4 Guide plate

The solar water heater equipped with guide plates in $\phi 58 \times 1\,800$ mm evacuated tube of high absorptivity is tested

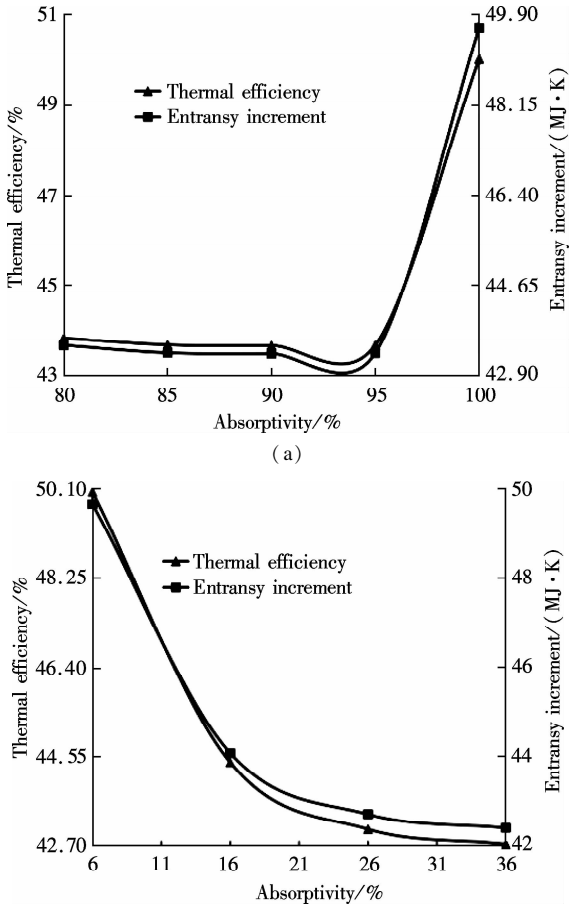

Fig. 4 Simulation analysis for absorptivity and emissivity. (a) Absorptivity; (b) Emissivity

and simulated to determine the effect of guide plates on the water heaters. As shown in Fig. 5, although the water heating rate of the tank with guide plates equipped in the tube is lower than that of the water heater without guide plates at the test beginning with stagnation and change in water, the average water temperature of a heater with guide plates is higher by a value ranging from 0.1 to 0.5 ℃ than that of the heater without guide plates with the increase in the irradiation time. The influence of length,

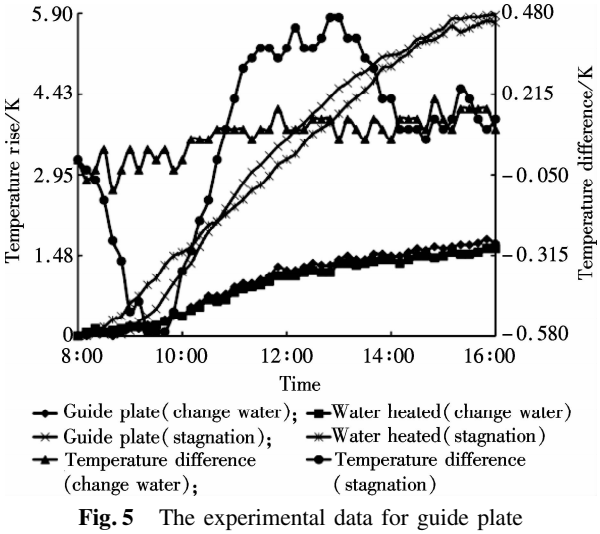

Fig. 5 The experimental data for guide plate

thickness and position of the guide plates on the thermal efficiency is simulated by using the above-developed mathematical model. As shown in Tab. 1, the reasonable guide plate length of the tube heated on a single surface is 50 to 100 mm from the bottom of the evacuated tube, but that of the tube heated on the double surface is 1 000 to 1 600 mm from the mouth of the evacuated tube. The water temperature decreases at first and then increases gradually with the guide plates extending toward the evacuated tube bottom. The reasonable plate length for the tube heated on the single surface is 1 740 mm while the reasonable one for the tube heated on the double surface is 1 500 mm. The reasonable position of the guide plates for both tubes is 15 to 20 mm above the tube central axis when the guide plates move along the radial direction.

Tab. 1 The reasonable length and position of guide plates

Specifications/mm	Single heated length/mm	Single heated position/mm	Double heated length/mm	Double heated position/mm
ϕ47 × 1 200	1 100	Above 16	1 070	Central
ϕ47 × 1 500	1 440	Above 16	1 070	Above 4
ϕ47 × 1 800	1 710	Above 16	1 480	Central
ϕ58 × 1 500	1 440	Above 20	1 200	Above 20
ϕ58 × 1 800	1 740	Above 20	1 500	Above 20
ϕ58 × 2 100	2 030	Above 20	1 600	Above 20

3 Field Synergy Analysis

The field synergy principle theoretically describes the synergy degree of flow and heat transfer, which employs the β angle to define the synergy degree of velocity vector and the temperature gradient vector. The field synergy principle is used to analyze the field synergy in the water heater with guide plates and that in the water heater with horizontal double collectors, as shown in Figs. 6 and 7.

3.1 Natural convective heat transfer

In Fig. 6(a), it is observed that the temperature layering is obvious in the water tank and it is more obvious at the bottom of the water tank. The β-angle values are 90° on the bottom of the water tank. Vertical flows and horizontal flows in the water tank are due to jet disturbance. Thermal fluid flows into the water tank along the evacuated tube wall. The β-angle values are 0° because the velocity vectors are consistent with the temperature gradient vectors. The cyclotron flow is formed in the evacuated tube by a natural convective heat transfer. The temperature at the bottom of the evacuated tube is higher than other areas because the stagnation zone reduces heat transfer. The temperature layering in the water tank is of uniform distribution and the temperature gradient vectors decrease after being equipped with guide plates. The flow in the evacuated tube is more uniform because the cyclotron flow disappears when the guide plate separates the cold and hot fluid, thus decreasing the stagnation area at the bottom of evacuated tubes.

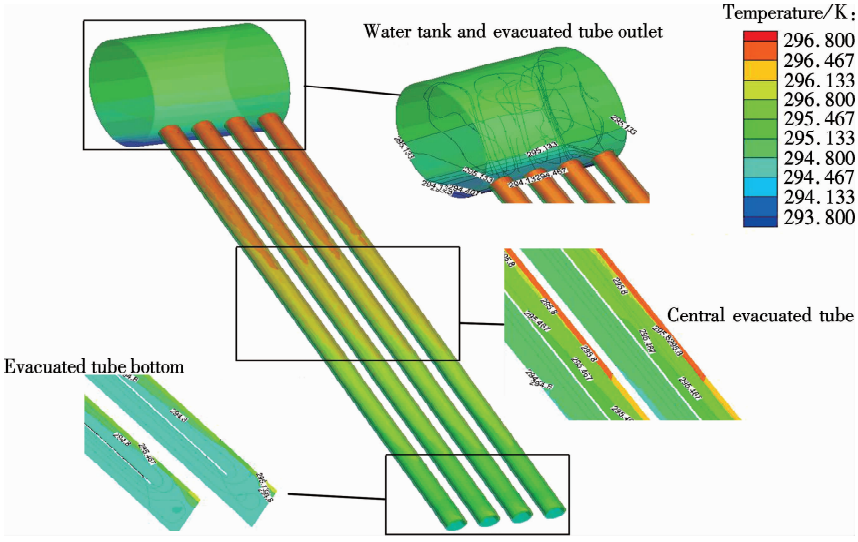

(a)

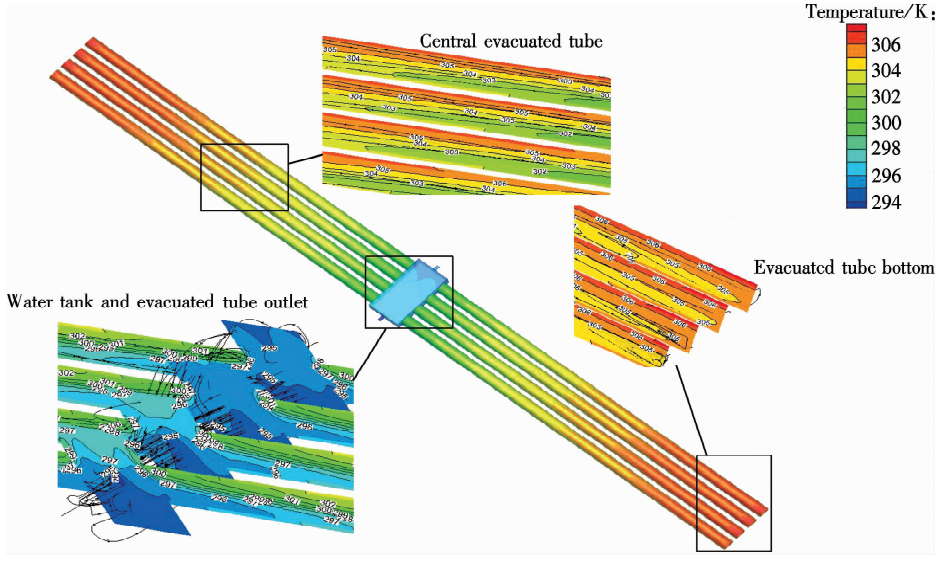

(b)

Fig. 6 Field synergy analysis. (a) For guide plate; (b) For horizontal double collector

3.2 Forced convective heat transfer

In Fig. 6(b), the β-angle values are 0° or 180° because the collector overall temperatures gradually decrease from the evacuated tube bottom to the manifold, which causes more fluid to absorb bottom heat, the internal flow of evacuated tube is smooth and the mixed flow in the evacuated tube disappears. The manifold velocity gradually decreases because there is backflow in the internal. The fluid temperature along the flow direction increases because fluid absorbs solar radiation. The field synergy in the collector outlet is greater than others because the temperature field is consistent with the velocity field according to the numerical simulation values.

4 Entransy Analysis

The entransy principle and entransy dissipation extreme principle are applied to analyze the enhancement of heat transfer in the water heaters according to Eqs. (9) and (10)[10-11]. The obtained results for the entransy dissipation for natural and forced convection heat transfers are shown in Fig. 7.

4.1 Natural convective heat transfer

As shown in Fig. 7(a), the entransy increment gradually rises with heating time. The entransy increment with double heated surfaces is larger than others. The entransy increment with the guide plate for the initial period is lower than that of the single heated surface, indicating that the guide plate improves the field synergy in the evacuated tube and reduces entransy dissipation. Entransy dissipation increases at first and then decreases because many backflows are formed in the evacuated tube by the double surfaces being heated. Entransy dissipation along the evacuated tube gradually increases and it is higher than others because the stagnation zone at the bottom of the evacuated tube is formed by the single surface being heated.

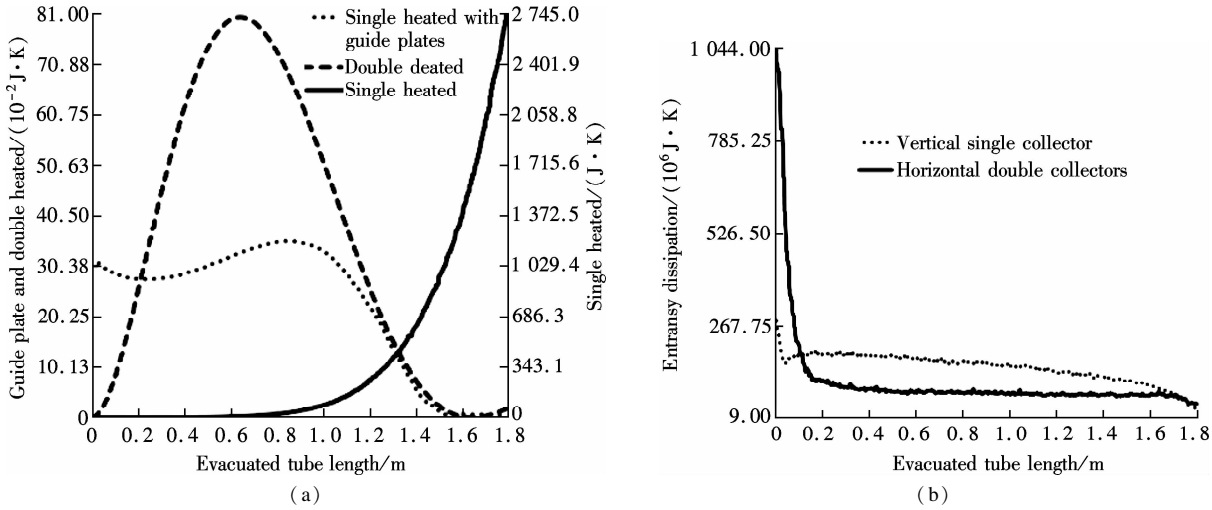

Fig. 7 Entransy dissipation. (a) For natural convection; (b) For forced convection

4.2 Forced convective heat transfer

Although entransy increments of vertical single and horizontal double collectors are negative values in the initial period, their entransy increments gradually increase with heating time. As shown in Fig. 7(b), the entransy dissipations of the vertical single collector and horizontal double collectors gradually decrease along the evacuated tube axial. The enhancement heat transfer effect of the horizontal double collectors is greater than that of the single vertical collector. The entransy increment of the horizontal double collectors is higher than that of single vertical collectors, but the entransy dissipation of the horizontal double collectors is lower than that of the single vertical collector.

5 Conclusion

The experiment and simulation of all-glass evacuated tube solar water heaters are conducted in the solar-assisted fuel cell system. The results show that the thermal performance of the water heater with a reflector is better than that of the ordinary water heater. The average temperature of the water tank gradually increases and the thermal efficiency decreases with tube diameter and length. The performance of the water heater is improved by increasing the absorptivity from 0.95 to 1.0 and decreasing the emissivity from 0.16 to 0.06. The entransy increment of horizontal double collectors is higher than that of the vertical single collector while the entransy dissipation is lower than that of the vertical single collector. It is concluded that the solar collectors with guide plates are suitable for natural convection while the double horizontal collectors are suitable for forced convection in the thermal field of solar-assisted fuel cell systems at low and medium temperatures.

References

[1] Pachauri R K, Chauhan Y K. A study, analysis and power management schemes for fuel cells[J]. *Renewable and Sustainable Energy Reviews*, 2015, **43**: 1301 – 1319. DOI:10.1016/j.rser.2014.11.098.

[2] Akikur R K, Saidur R, Ping H W, et al. Performance analysis of a co-generation system using solar energy and SOFC technology[J]. *Energy Conversion and Management*, 2014, **79**: 415 – 430. DOI:10.1016/j.enconman.2013.12.036.

[3] Behzadi M S, Niasati M. Comparative performance analysis of a hybrid PV/FC/battery stand-alone system using different power management strategies and sizing approaches[J]. *International Journal of Hydrogen Energy*, 2015, **40**(1): 538 – 548. DOI:10.1016/j.ijhydene.2014.10.097.

[4] Morrison G L, Budihardjo I, Behnia M. Water-in-glass evacuated tube solar water heaters[J]. *Solar Energy*, 2004, **76**(1/2/3): 135 – 140. DOI:10.1016/j.solener.2003.07.024.

[5] Morrison G L, Budihardjo I, Behnia M. Measurement and simulation of flow rate in a water-in-glass evacuated tube solar water heaters[J]. *Solar Energy*, 2005, **78**(2): 257 – 267. DOI:10.1016/j.solener.2004.09.005.

[6] Yan S Y, Tian R, Yu W Y. Analysis on factors influencing fluid flow in an all-glass evacuated tube solar water heaters[J]. *Journal of Engineering Thermophysics*, 2010, **31**(4):641 – 643. (in Chinese)

[7] Yan S Y, Huang H Y, Tian R. Mechanism analysis for the heat transfer enhancement with all-glass evacuated tube solar water heaters[J]. *Journal of Engineering Thermophysics*, 2012, **33**(3):485 – 488. (in Chinese)

[8] Budihardjo I, Morrison G L. Performance of water-in-glass evacuated tube solar water heaters[J]. *Solar Energy*, 2009, **83**(1): 49 – 56. DOI:10.1016/j.solener.2008.06.010.

[9] Zhang X Y, You S J, Xu W, et al. Experimental investigation of the higher coefficient of thermal performance for water-in-glass evacuated tube solar water heaters in China[J]. *Energy Conversion and Management*, 2014, **78**: 386 – 392. DOI:10.1016/j.enconman.2013.10.070.

[10] Guo Z Y, Tao W Q, Shah R K. The field synergy (coordination) principle and its applications in enhancing single phase convective heat transfer[J]. *International Jour-*

nal of Heat and Mass Transfer, 2005, **48**(9): 1797 - 1807. DOI:10.1016/j.ijheatmasstransfer.2004.11.007.

[11] Guo Z Y, Zhu H Y, Liang X G. Entransy—a physical quantity describing heat transfer ability[J]. *International Journal of Heat and Mass Transfer*, 2007, **50**(13/14): 2545 - 2556. DOI:10.1016/j.ijheatmasstransfer.2006.11.034.

全玻璃真空管太阳能集热器流动换热的试验和数值模拟

张 涛 韩吉田 陈常念 孔令健 刘 洋

(山东大学能源与动力工程学院, 济南 250061)

摘要:以太阳能与燃料电池耦合系统为应用背景,对不同管长和管径、不同吸收率和发射率和有/无内置导流板3种不同情况下的太阳能集热器进行试验研究.建立太阳能集热器自然对流和强迫对流数值计算模型,并应用场协同和火积理论分析模拟计算数据.自然对流研究表明,随着真空管长度的增加,水箱温度逐渐升高,但集热效率逐渐下降;当吸收率在0.95~1.0范围内升高,发射率在0.16~0.06范围内降低时,集热效率逐渐上升;全玻璃真空管加装导流板后,由于真空管中混流消失和真空管底部强化传热作用而提高了太阳能集热器的热效率.强迫对流研究表明,横双排太阳能集热器的雷诺数、努赛尔数和火积增量均高于竖直单排太阳能集热器;横双排太阳能集热器的火积耗散低于竖直单排太阳能集热器.研究结果表明,在中低温太阳能耦合燃料电池集热场,自然对流宜采用内置导流板太阳能集热器,强迫对流宜采用横双排太阳能集热器.

关键词:全玻璃真空管太阳能集热器; 太阳能耦合燃料电池; 场协同; 火积耗散

中图分类号:TK515